BIBECHANA
ISSN 2091-0762 (Print), 2382-5340 (Online)
Journal homepage: http://nepjol.info/index.php/BIBECHANA
Publisher: Department of Physics, Mahendra Morang A.M. Campus, TU, Biratnagar, Nepal

Electronic and magnetic properties of defected MoS_2 monolayer

Hari Krishna Neupane[1, 2], Narayan Prasad Adhikari[2*]
[1]Amrit Campus, Institute of Science and Technology Tribhuvan University, Kathmandu, Nepal
[2]Central Department of Physics, Institute of Science and Technology Tribhuvan University, Kathmandu, Nepal
[*]Email: narayan.adhikari@cdp.tu.edu.np

Article Information:
Received: December 28, 2020
Accepted: April 17, 2021

Keywords:
DFT
Magnetic moment
Monolayer
Spins
Vacancy defects

ABSTRACT

It is interesting to understand the effect of defects in 2D materials, because vacancy defects in 2D materials have novel electronic and magnetic properties. In this work, we studied electronic and magnetic properties of 1S vacancy defect ($1S_v$-MoS_2), 2S vacancy defects ($2S_v$-MoS_2), 1Mo vacancy defect (Mo_v-MoS_2), and (1Mo & 1S) vacancy defects ($(Mo\text{-}S)_v$-MoS_2) in 2D MoS_2 material by first-principles calculations within spin-polarized density functional theory (DFT) method. To understand the electronic properties of materials, we have analyzed band structures and DOS calculations, and found that $1S_v$-MoS_2 & $2S_v$-MoS_2 materials have semiconducting nature. This is because, $1S_v$-MoS_2 & $2S_v$-MoS_2 materials open small energy band gap of values 0.68 eV & 0.54 eV respectively in band structures. But, in Mo_v-MoS_2 & $(Mo\text{-}S)_v$-MoS_2 materials, energy bands around the Fermi level mix with the orbital's of Mo and S atoms. As a result, bands are split and raised around and above the Fermi energy level. Therefore, Mo_v-MoS_2 & $(Mo\text{-}S)_v$-MoS_2 materials have metallic nature. We found that MoS_2, $1S_v$-MoS_2 & $2S_v$-MoS_2 materials have non-magnetic properties, and Mo_v-MoS_2 & $(Mo\text{-}S)_v$-MoS_2 materials have magnetic properties because magnetic moment of MoS_2, $1S_v$-MoS_2 & $2S_v$-MoS_2 materials have 0.00 μ_B/cell value and Mo_v-MoS_2 & $(Mo\text{-}S)_v$-MoS_2 materials have 2.72 μ_B/cell & 0.99 μ_B/cell respectively. Therefore, non-magnetic MoS_2 changes to magnetic Mo_v-MoS_2 & $(Mo\text{-}S)_v$-MoS_2 materials due to Mo and (1Mo & 1S) vacancy defects. Magnetic moment obtained in Mo_v-MoS_2 & $(Mo\text{-}S)_v$-MoS_2 materials due to the distribution of up and down spins in 4p, 4d & 5s orbitals of Mo atoms and 3s & 3p orbitals of S atoms in structures. The significant values of magnetic moment are given by distributed spins in 4d orbital of Mo atoms and 3p orbital of S atoms.

DOI: https://doi.org/10.3126/bibechana.v18i2.33905

1. Introduction

Two dimensional (2D) materials with atomic thickness have become candidates for wearable electronic devices in the future. Graphene and transition metal sulfides have received extensive attention in logic computing and sensing applications due to their lower power dissipation [1-3]. However, the lack of intrinsic band gap and non-magnetic nature of graphene limits its practical applications in widely expanding field of carbon-based devices. Therefore, the transition metal dichalcogenides material (TMD) Molybdenum diSulphide (MoS_2) is a suitable candidate for logic computing (logic computing is the sequence of operations (hardware or software) performed by computers) and sensing (devices) applications. MoS_2 is made by Mo and S atoms stacked together to give S-Mo-S in a triangular prismatic arrangement [4]. The band structure of MoS_2 depends on the number of layers, and the single layer MoS_2 has a direct band gap of energy 1.80 eV [5]. The band is opened in between the lower energy band of conduction band and higher energy band of valence band. Due to the wide band gap (1.80 eV), MoS_2 provides huge opportunities for electrical and optoelectronics [6-9]. In recent years, a lot of research has been carried out surrounding MoS_2, and various new electronic devices based on MoS_2 have emerged, including gas sensors, resistive memory, photo detectors, integrated logic circuits, signal amplifiers, flexible optoelectronic devices, solar cells and lubricants etc. [10-13].

Electronic and magnetic properties of 2D pristine and defected materials are attracting properties in solid-state physics because they have potential applications in industrial as well as academic sectors. Hence, it is interesting to understand the effect of defects in 2D materials [14-16]. The vacancy defects in solids causes deviation of atoms or ions from the periodicity and they are used to find innovative properties. They can be used to design new materials [17]. To our best knowledge, Mo and S atoms vacancy defects (i.e. 1Mo atom only, 1Mo and 1S atoms together) in monolayer MoS_2 material have not been reported [5, 18-21]. These Mo and S atoms vacancy defects in MoS_2 may provide significance outline for the material in device applications. Therefore, in this work, we focus on the electronic and magnetic properties of Mo and S atoms vacancy defects in monolayer MoS_2 through first-principles calculations within the frame work of density functional theory (DFT), using computational tool quantum ESPRESSO.

The remaining part of this paper is arranged as follows. In section 2, we introduce the computational details. Main finding and their interpretation are presented in section 3. Finally we draw conclusions in section 4.

2. Computational Methods

In this work, we used spin-polarized density functional theory (DFT) [22], with the quantum ESPRESSO simulation package [23] and structure visualization program XCrySDen [24], to perform all the calculations. The Generalized Gradient Approximation (GGA) of Perdew-Burke-Ernzerhof (PBE) [25] is used to describe the exchange correlation interactions. The Rappe-Rabe-Kaxiraas-Joannopoulos (RRKJ) model of ultra-soft pseudo-potentials is used to describe chemically active valence electrons in calculations. The kinetic energy cut-off and charge density cut-off values are set to 35 Ry and 350 Ry respectively for the plane-wave expansion. The first Brillouin zone is sampling of a (10×10×1) Monkhorst-Pack (MP) [26] k-points grid, which is used to perform geometric optimizations. All the structures are fully relaxed by Broyden-Fletcher-Goldfarb-Shanno (BFGS) scheme [27], until the energy and force are converged less than 10^{-4} Ry and 10^{-3} Ry/Bohr values respectively. The mesh of (6×6×1) k-points grid is used to perform all bands structure calculations and automatic denser mesh (12×12×1) k-points is used for density of states (DoS) and partial density of states (PDoS) calculations, where in both the cases, 100 k-points are chosen along the high symmetric points connecting the reciprocal space. The Marzarri-Vanderbilt (MV) [28]

smearing of small width 0.001 Ry is used. In addition, we have chosen 'david' diagonalization method with 'plain' mixing mode and mixing factor of 0.6 for self consistency.

In present work, we have constructed (3×3) supercell structure of monolayer MoS_2 from the unit cell by extending along x and y direction as shown in figure 1(a). Then, we have generated stable and relaxed structures of 1S vacancy defect in MoS_2 ($1S_v$-MoS_2), 2S vacancy defects in MoS_2 ($2S_v$-MoS_2), 1Mo vacancy defect in MoS_2 (Mo_v-MoS_2) and (1Mo & 1S) vacancy defects in MoS_2 $(Mo\text{-}S)_v$-MoS_2 materials as shown in figures 1(b-i). These prepared structures are used for further investigations.

3. Results and Discussion

In this section, we reported first-principles calculations within the frame work of spin-polarized DFT method to study electronic and magnetic properties of Mo and S atoms vacancy defects in MoS_2 material.

3.1 Electronic Properties

The electronic properties of $1S_v$-MoS_2, $2S_v$-MoS_2, Mo_v-MoS_2 and $(Mo\text{-}S)_v$-MoS_2 materials are studied by the analysis of band structures and DoS calculations using DFT method. The optimized and relaxed structures of MoS_2, $1S_v$-MoS_2, $2S_v$-MoS_2, Mo_v-MoS_2 and $(Mo\text{-}S)_v$-MoS_2 materials are shown in figures 1(a-i) respectively. Before study the band structures and DoS calculations of $1S_v$-MoS_2, $2S_v$-MoS_2, Mo_v-MoS_2 and $(Mo\text{-}S)_v$-MoS_2 materials, we need to understand the electronic properties of pure MoS_2 material. We know that the electronic configurations of valence electrons in Mo and S atoms are [Kr] $4d^5\ 5s^1$ and [Ne] $3s^2\ 3p^4$ respectively. A hexagonal unit cell of monolayer MoS_2 on the basis of three (1Mo & 2S) atoms in honeycomb lattice structure is initially constructed by using reported value [29, 30]. It is built up by single layers of S-Mo-S atoms. It consists of two planes of Sulphur (S) atoms and an intercalated plane of Molybdenum (Mo) atom which bounds with the Sulphur atoms in a trigonal prismatic arrangement. Each Mo atom is surrounded by six first nearest neighboring S atoms. Based on convergence test, we obtained the lattice constant 'a' for MoS_2 equals to 3.137Å, which agrees with the reported value 3.19Å [31]. The (3×3) supercell structure of monolayer MoS_2 is constructed by using the lattice constant which is three times that of the unit cell as shown in figure 1(a).

We have done band structure calculations of MoS_2 supercell structure, and obtained band gap energy value 1.23 eV, this value is close to reported value 1.80 eV [26]. Therefore, we also concluded that monolayer MoS_2 is a wide band gap semiconductor. The band structure of monolayer MoS_2 is shown in figure 2(a), where x-axis represents high symmetric points in the first Brillouin zone and y-axis represents the corresponding energy values.

In addition, we have prepared stable and relaxed structures of $1S_v$-MoS_2, $2S_v$-MoS_2, Mo_v-MoS_2 and $(Mo\text{-}S)_v$-MoS_2 by removing 1S, 2S, 1Mo and (1Mo & 1S) atoms in supercell structure of MoS_2, with defects formation energy 0.52 eV, 0.76 eV, 0.64 eV and 0.87 eV respectively. These defects formation energy are calculated by using the standard formalism [32];

$$E_d = E_{T\text{-}d} - (E_{T\text{-}p} + n_d\mu_d) \quad \ldots (1)$$

where, $E_{T\text{-}d}$ is a total energy of a supercell with the defects, n_d, is the numbers of atom removed from the perfect super cell to introduce a vacancy, μ_d is chemical potentials of defected atom in structures, $E_{T\text{-}p}$ is the total energy of the neutral perfect supercell respectively. Defects formation energy values of these materials are given in table 1. The stability of these structures is observed by binding energy calculations. Higher the value of binding energy means, systems are more stable. The binding energy of materials depends upon calculated total energy of the systems, which are also given in table 1.

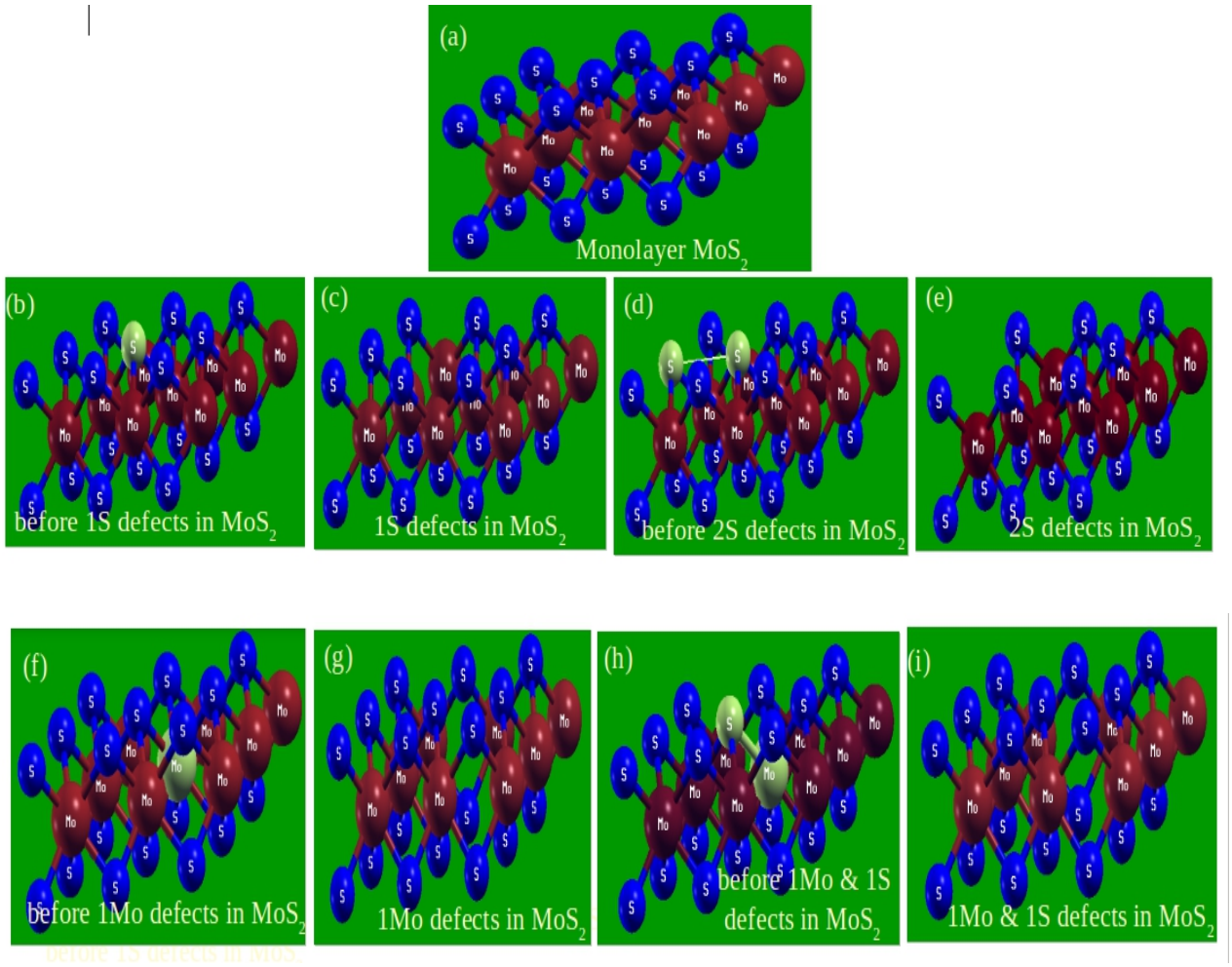

Fig. 1: (a) (3×3) supercell structure of monolayer MoS_2 (b) Before 1S vacancy defect in (3×3) supercell structure of monolayer MoS_2 (c) 1S vacancy defect in (3×3) supercell structure of monolayer MoS_2 (d) before 2S vacancy defects in (3×3) supercell structure of monolayer MoS_2 (e) 2S vacancy defects in (3×3) supercell structure of monolayer MoS_2 (f) Before 1Mo vacancy defect in (3×3) supercell structure of monolayer MoS_2 (g) 1Mo vacancy defect in (3×3) supercell structure of monolayer MoS_2 (h) Before 1Mo & 1S vacancy defects in (3×3) supercell structure of monolayer MoS_2 (i) 1Mo & 1S vacancy defects in (3×3) supercell structure of monolayer MoS_2.

We calculated the inter-atomic distances of atoms in pristine and defected MoS_2 monolayer. It is found that compactness of the materials is decreased due to vacancy defects in structure. This is because, inter-atomic bondings are broken due to vacancy defect atom (atoms) in structures, and remaining atoms are loosely bounded to each other. The inter–atomic distances in pristine and vacancy defected MoS_2 materials are given in table 2.

Table 1: Fermi energy (E_f), Fermi energy shift (E_s), bandgap energy (E_g), total energy of system (E_t), defects formation energy (E_d), total value of magnetic moment (M), and magnetic moment due to total up & down spins states of electrons (μ) in 4p, 4d & 5s orbitals of Mo atoms; 3s & 3p orbitals of S atoms in $1S_v$-MoS_2, $2S_v$-MoS_2, Mo_v-MoS_2, and $(Mo\text{-}S)_v$-MoS_2 materials.

Data of band structures, DoS and PDoS calculations of MoS_2, S_v-MoS_2, Mo_v-MoS_2 & $(Mo\text{-}S)_v$-MoS_2 materials	MoS_2	$1S_v$-MoS_2	$2S_v$-MoS_2	Mo_v-MoS_2	$(Mo\text{-}S)_v$-MoS_2
E_f (eV)	-1.89	-1.97	-2.02	-2.30	-2.33
E_s (eV)	-	0.08	0.13	0.41	0.44
E_g (eV)	1.23	0.68	0.54	-	-
E_t (Ry)	-1741.61	-1718.60	-1696.58	-1593.42	-1570.53
E_d (eV)	---	0.52	0.76	0.64	0.87
μ due to 4p of Mo atoms (μ_B/cell)	0.00	0.00	0.00	0.03	0.01
μ due to 4d of Mo atoms (μ_B/cell)	0.00	0.00	0.00	0.73	0.23
μ due to 5s of Mo atoms (μ_B/cell)	0.00	0.00	0.00	0.03	0.01
μ due to 3s of S atoms (μ_B/cell)	0.00	0.00	0.00	0.04	0.02
μ due to 3p of S atoms (μ_B/cell)	0.00	0.00	0.00	1.89	0.72
T Total value of magnetic moment M (μ_B/cell)	0.00	0.00	0.00	2.72	0.99

Table 2: Inter-atomic distances in pristine MoS_2 and vacancy defects MoS_2 materials, where S-S, Mo-Mo and Mo-S represent inter-atomic bonding in between any two neighbouring Sulphur atoms, any two Molybdenum atoms and nearest neighbour 1Mo and 1S atoms in structures.

Inter-atomic distances of pristine MoS_2 and defected MoS_2 monolayer along x, y and z axis	x-axis (Å)			y-axis (Å)			z-axis (Å)		
	S–S	Mo-Mo	Mo-S	S-S	Mo-Mo	Mo-S	S-S	Mo-Mo	Mo-S
Pristine MoS_2	0.00	1.57	1.52	0.00	2.74	0.90	3.13	0.00	1.56
1S defect MoS_2	0.00	1.57	1.54	0.00	2.74	0.91	3.14	0.00	1.57
2S defects MoS_2	0.00	1.58	1.56	0.00	2.75	0.92	3.15	0.00	1.58
1Mo defect MoS_2	0.00	1.61	1.58	0.00	2.78	0.95	3.15	0.03	1.60
1Mo & 1S defects MoS_2	0.02	1.62	1.59	0.02	2.78	0.97	0.01	0.03	0.62

We have done band structures calculations of $1S_v$-MoS_2, $2S_v$-MoS_2, Mo_v-MoS_2 and $(Mo\text{-}S)_v$-MoS_2 materials as shown in figures 2(b-e) respectively, where 100 k-points are taken along the specific direction of irreducible Brillouin zone by choosing Γ-M-K-Γ high symmetric points. Also, high symmetric points in the first Brillouin zone are taken along x-axis and corresponding energies are taken along y-axis.

The $1S_v$-MoS_2 and $2S_v$-MoS_2 materials have opened narrow band gap of values 0.68 eV and 0.54 eV respectively as shown in figures 2(b-c). Hence, the materials resemble with the nature of semiconductors. The band gap energy value of defected materials decreases with increase in defects concentrations in MoS_2 structure, which determines the conductivity strength of materials. Thus, the strength of conductivity in $2S_v$-MoS_2 is greater than $1S_v$-MoS_2. Also, conductivity of defected materials is higher than non-defected monolayer MoS_2 supercell structure. On the other hand, bands states of Mo_v-MoS_2 and $(Mo\text{-}S)_v$-MoS_2 materials split and cross the Fermi energy level as shown in figures 2(d-e) respectively. Bands around Fermi level mix with the orbital's of Mo vacancy in Mo_v-MoS_2, and (1Mo & 1S) vacancies in $(Mo\text{-}S)_v$-MoS_2. The states associated with the dangling bond and reconstructed Mo-S bond of vacancy occurs near the top of valence band and in conduction band, and appear as flat bands as shown in figures 2(d) and 2(e). Therefore, from the band calculations, Mo_v-MoS_2 and $(Mo\text{-}S)_v$-MoS_2 materials have metallic nature. The vacancies position of S and Mo atoms in structures creates unpaired spins of electrons in sub-orbitals of Mo-S atoms in structures. We have calculated the Fermi energy of $1S_v$-MoS_2, $2S_v$-MoS_2, Mo_v-MoS_2 and $(Mo\text{-}S)_v$-MoS_2 materials and found -1.97 eV, -2.02 eV, -2.30 eV and -2.33 eV values respectively. These obtained different values of Fermi energy are, due to unpaired total up & down spins states of electrons and movement of charges carriers in structures.

We have analyzed DoS and PDoS calculations for the investigation of magnetic properties in materials. Figures 3(a) and 3(b) represent DoS and PDoS plots of pure monolayer MoS_2; figures 4(a) and 4(b) represent total DoS plots of S_v-MoS_2 and $2S_v$-MoS_2 materials, figures 4(c) and 4(d) represent total PDoS plots of $1S_v$-MoS_2 and $2S_v$-MoS_2 materials, figures 5(a) and 5(b) represent total DoS plots of Mo_v-MoS_2 and $(Mo\text{-}S)_v$-MoS_2 materials, and figures 5(c) and 5(d) represent total PDoS plots of Mo_v-MoS_2 and $(Mo\text{-}S)_v$-MoS_2 materials respectively, where the states above the horizontal line represents up spin states of electrons and a state below the horizontal line represents down spin states of electrons.

3.2 Magnetic Properties

The induced magnetization in the materials is obtained by analysis of DoS and PDoS calculations of materials. The asymmetrically distributed up and down spins states of electrons in DoS and PDoS plots reflect, materials have magnetic properties, and symmetrically distributed up and down spins states of electrons in DoS and PDoS plots means, materials carry non-magnetic properties. Up and down spins states of electrons in the orbitals of Mo & S atoms are symmetrically distributed in DoS and PDoS plots of MoS_2, $1S_v$-MoS_2 and $2S_v$-MoS_2 materials are shown in figures 3(a) & 3(b), figures 4(a) & 4(c), and 4(b) & 4(d) respectively. Magnetic moment due to up and down spins states of electrons in 4p, 4d & 5s orbitals of Mo atoms and 3s & 3p orbitals of S atoms in MoS_2, $1S_v$-MoS_2 and $2S_v$-MoS_2 have value 0.00 μ_B/cell, which are given in table 1. Therefore, MoS_2, $1S_v$-MoS_2 and $2S_v$-MoS_2 materials have non-magnetic properties.

We have investigated magnetic properties of Mo_v-MoS_2 and $(Mo\text{-}S)_v$-MoS_2 materials from the DoS and PDoS calculations using spin-polarized DFT method. The DoS and PDoS of up and down spins states of electrons near the Fermi level are asymmetrically distributed in Mo_v-MoS_2 material as shown in figures 5(a) & 5(c) respectively.

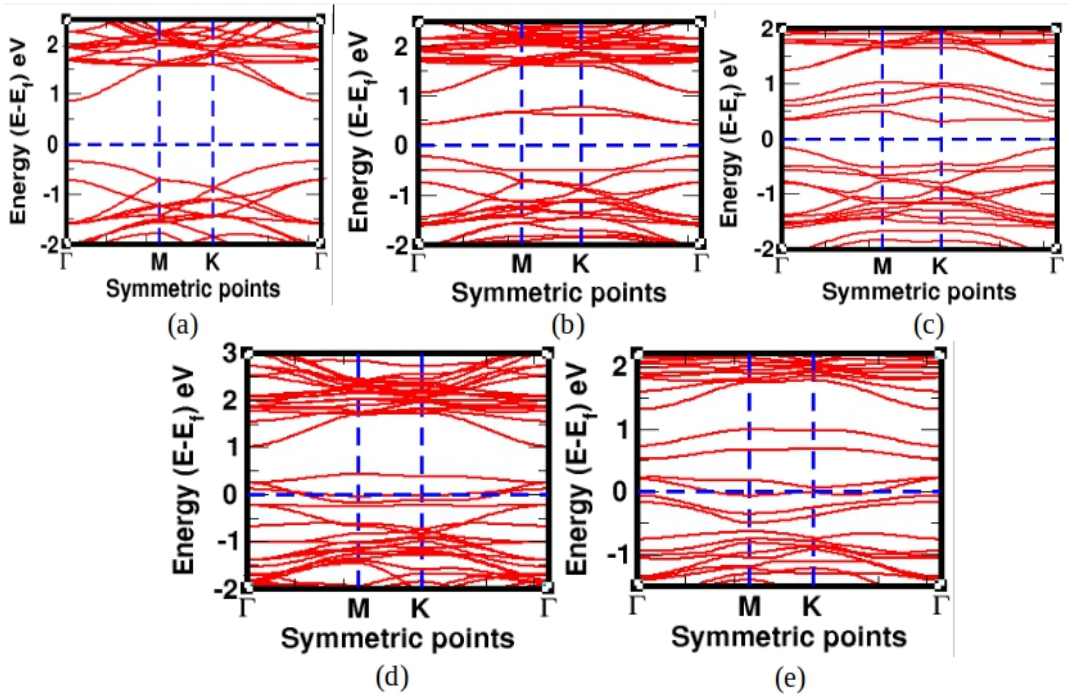

Fig. 2: (a) Band structure of monolayer MoS_2 (b) Band structure of 1S vacancy defect in monolayer MoS_2 (c) Band structure of 2S vacancy defects in monolayer MoS_2 (d) Band structure of 1Mo vacancy defect in monolayer MoS_2 (e) Band structure of (1Mo & 1S) vacancy defects in monolayer MoS_2. In all band structure plots, horizontal dotted line represents Fermi energy level.

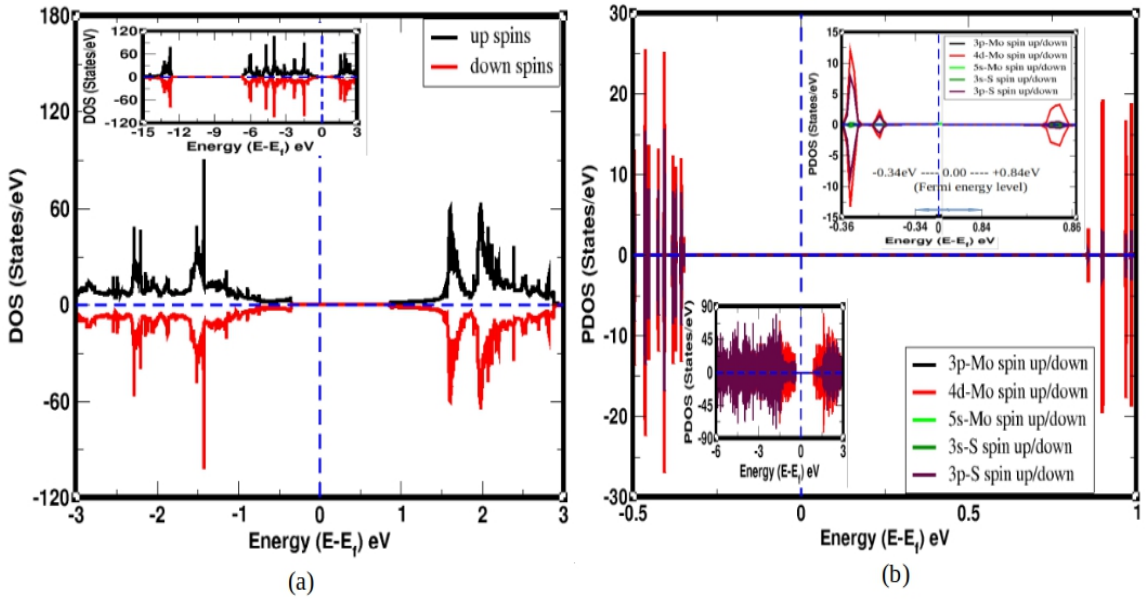

Fig. 3: (a) Total DoS of (3×3) supercell structure of monolayer MoS_2 (b) PDoS of up and down spins states of electrons in the individual orbitals of Mo & S atoms in (3×3) supercell structure of MoS_2 material. In DoS and PDoS plots, vertical dotted line represents Fermi energy level.

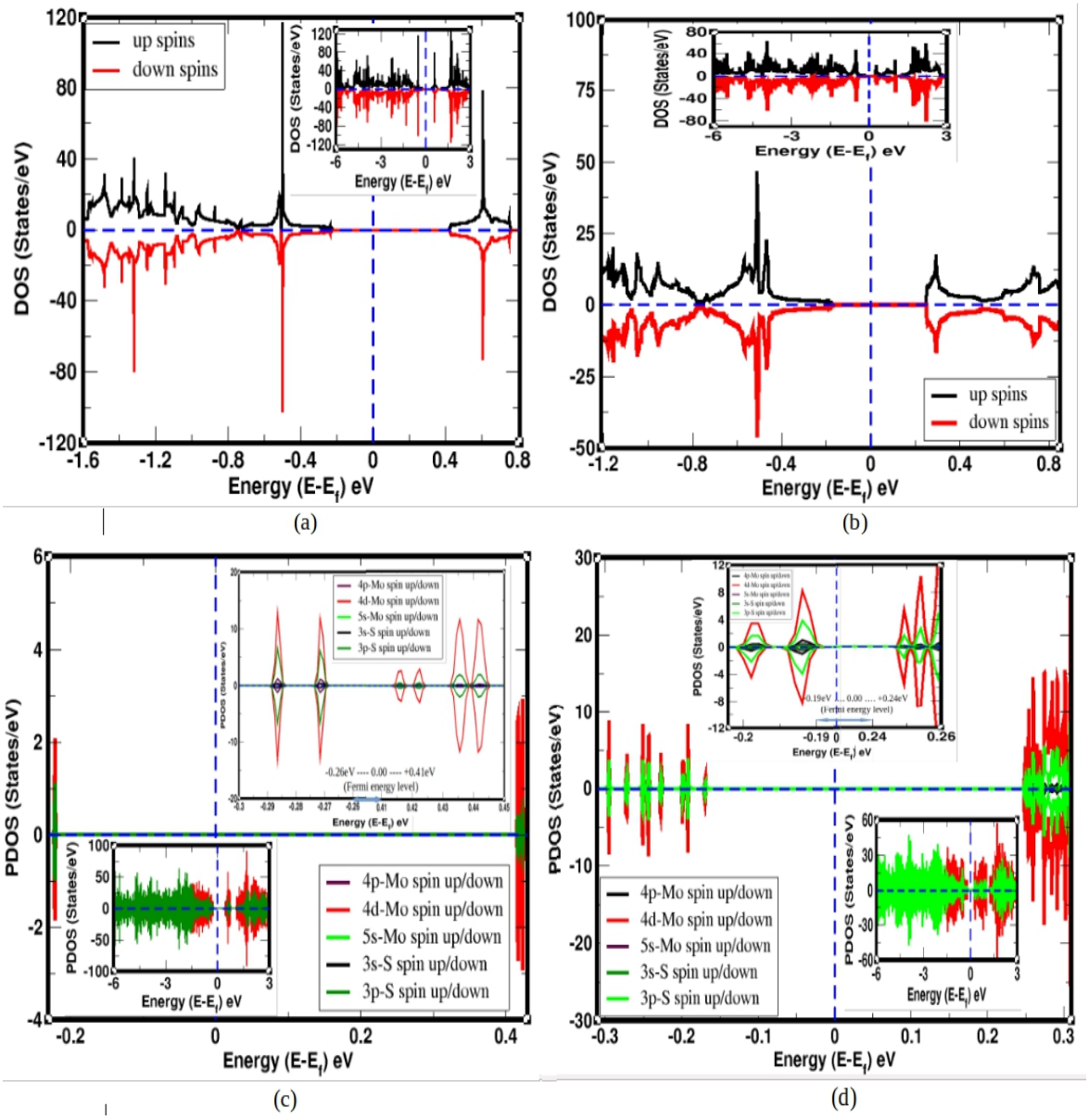

Fig. 4: (a) Total DoS of up & down spins states of electrons in the orbitals of Mo & S atoms in 1S vacancy defect in MoS_2 material (b) Total DoS of up & down spins states of electrons in the orbitals of Mo & S atoms in 2S vacancy defects in MoS_2 material (c) PDoS of up & down spins states of electrons in the individual orbital of Mo & S atoms in 1S vacancy defect MoS_2 material (d) PDoS of up & down spins states of electrons in the individual orbital of Mo & S atoms in 2S vacancy defects MoS_2 material. In DoS and PDoS plots, vertical dotted line represents Fermi energy level.

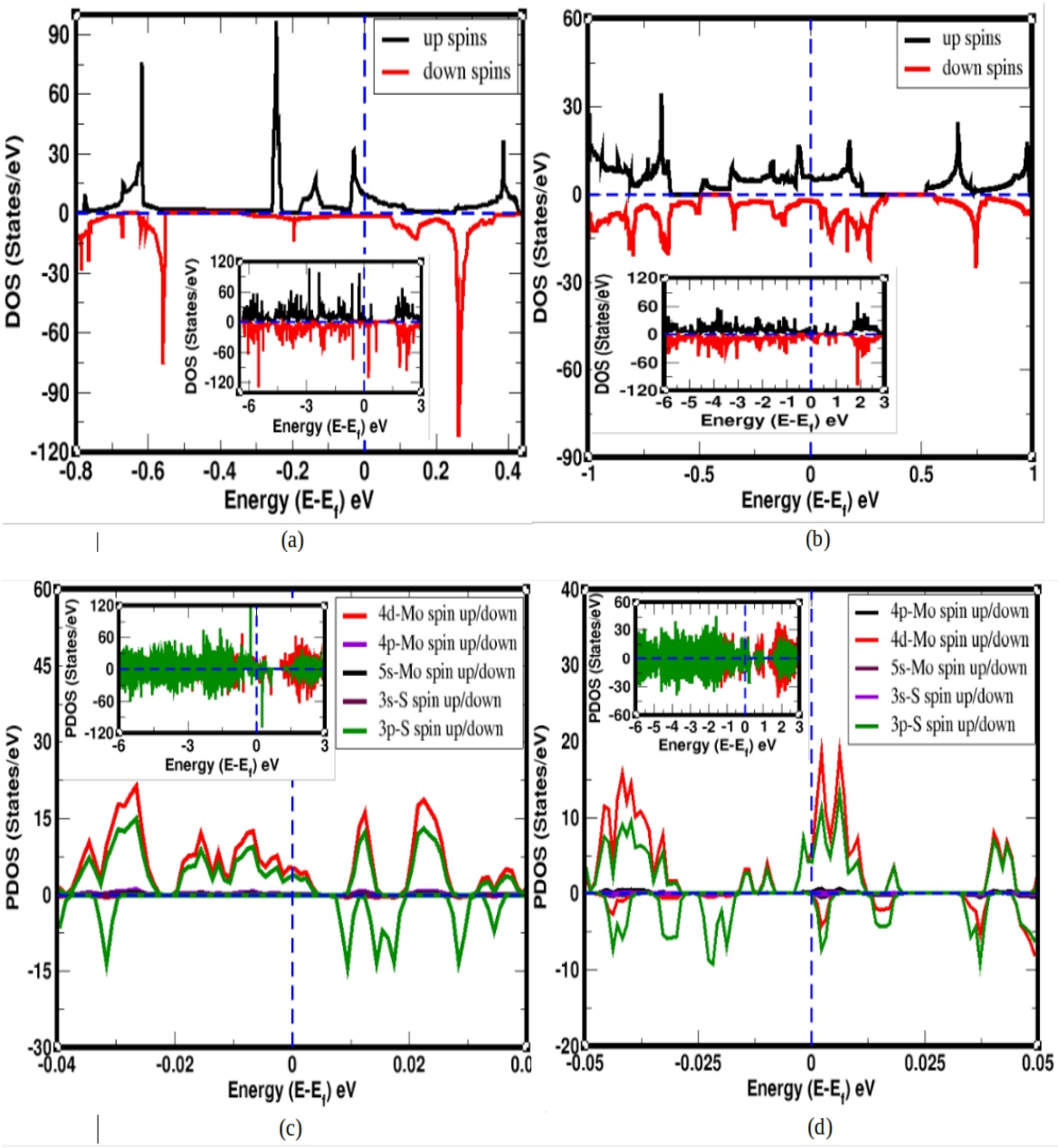

Fig. 5: (a) Total DoS of up & down spins states of electrons in the orbitals of Mo & S atoms in 1Mo vacancy defect in MoS_2 material (b) Total DoS of up & down spins states of electrons in the orbitals of Mo & S atoms in (1Mo & 1S) atoms vacancy defects MoS_2 material (c) PDoS of up & down spins states of electrons in the individual orbital of Mo & S atoms in 1Mo vacancy defect in MoS_2 material (d) PDoS of up & down spins states of electrons in the individual orbital of Mo & S atoms in (1Mo & 1S) atoms vacancy defects MoS_2 material. In DoS and PDoS plots, vertical dotted line represents Fermi energy level.

This is because, electron's spins degeneracy of the bands due to Mo vacancy defects, bands are broken and splited. As a result, Mo_v-MoS_2 material bears magnetic properties. We have also calculated the magnetic moments given by spins of electrons in 4p, 4d & 5s orbitals of Mo atoms and 3s & 3p orbitals of S atoms having values 0.03 μ_B/cell, 0.73 μ_B/cell & 0.03 μ_B/cell; and 0.04 μ_B/cell & 1.89

μ_B/cell in Mo_v-MoS_2 material respectively. Hence, total value of magnetic moment in Mo_v-MoS_2 material is 2.72μ_B/cell. From above calculations, we know that spins states of electrons in 4d orbital of Mo atoms, and 3p orbital of S atoms have dominant contributions for magnetism. Similarly, the spins states of electrons in the orbital of Mo & S atoms of $(Mo\text{-}S)_v$-MoS_2 material near the Fermi energy level are asymmetrically distributed in DoS and PDoS plots as shown in figures 5(b) & 5(d) respectively. Magnetic moment is given by spins states of electrons in 4p, 4d & 5s orbitals of Mo atoms; and 2s & 2p orbitals of S atoms; in structure have values 0.01 μ_B/cell, 0.23 μ_B/cell & 0.01 μ_B/cell; and 0.02 μ_B/cell & 0.72 μ_B/cell respectively. The total magnetic moment in $(Mo\text{-}S)_v$-MoS_2 material has value 0.99 μ_B/cell. Therefore, $(Mo\text{-}S)_v$-MoS_2 material has magnetic properties. 4d orbital of Mo and 3p orbital of S atoms give greater values of magnetic moment than magnetic moment given by other orbitals of atoms in the material. Magnetic moment of Mo_v-MoS_2 is higher than that of $(Mo\text{-}S)_v$-MoS_2 material because unequal unpaired (dangling) bonds are present in structures. These dangling bonds are formed due to the effects of 1Mo atom vacancy defects and (1Mo & 1S) atoms vacancy defects in the materials. It is also seen that spins polarization of atoms in (1Mo &1S) atoms vacancy defects structure is less than 1Mo atom vacancy defects structure.

4. Conclusions and Concluding Remarks

The novel properties in MoS_2 material are developed due to Mo and S atoms vacancy defects. The electronic and magnetic properties of $1S_v$-MoS_2, $2S_v$-MoS_2, Mo_v-MoS_2 and $(Mo\text{-}S)_v$-MoS_2 materials are studied through first-principles calculations within the frame work of spin-polarized DFT method using computational tool quantum ESPRESSO. We have prepared stable structures of these materials, and then analyzed their band structures, DoS and PDoS calculations. From the band structure calculations, we found that $1S_v$-MoS_2 and $2S_v$-MoS_2 materials have open small energy band gap of value 0.68 eV and 0.58 eV in both up and down spins electronic states, which implies that $1S_v$-MoS_2 and $2S_v$-MoS_2 resemble with the nature of semiconductors. Thus, conductivity of material increases with increase in its defects concentrations. On the other hand, Mo_v-MoS_2 and $(Mo\text{-}S)_v$-MoS_2 materials have metallic properties because bands around the Fermi level mix with the orbital's of Mo vacancy in Mo_v-MoS_2, and (Mo & S) vacancies in $(Mo\text{-}S)_v$-MoS_2. The states associated with the dangling bond and reconstructed Mo-S bond of vacancy occurs near the top of valence band and in conduction band, and appear as flat bands. The charge densities associated in these bands are localized. From the analysis of DoS and PDoS calculations, we found that MoS_2, $1S_v$-MoS_2 and $2S_v$-MoS_2 materials have non-magnetic properties. The non-magnetic MoS_2 material changes to magnetic Mo_v-MoS_2 and $(Mo\text{-}S)_v$-MoS_2 materials, due to 1Mo atom vacancy defects in monolayer MoS_2 and (1Mo & 1S) atoms vacancy defects in monolayer MoS_2 structure respectively. Total magnetic moment of Mo_v-MoS_2 and $(Mo\text{-}S)_v$-MoS_2 materials have values 2.72 μ_B/cell and 0.99 μ_B/cell respectively. Significant values of magnetic moment are obtained due to the distribution of electrons spins in 4p, 4d, & 5s orbitals of Mo atoms and 3s & 3p orbitals of S atoms in both materials.

Acknowledgments

Hari Krishna Neupane and Narayan Prasad Adhikari acknowledge the UGC Nepal award no. PhD-75/76-S&T-09 and grants CRG 073/74 -S&T -01 respectively. Also, Narayan Prasad Adhikari acknowledges network project NT-14 of ICTP/OEA.

References

[1] J. C. Lei, X. Zhang, and Z. Zhou, Recent advances in MXene: Preparation, properties, and applications, Frontiers of Physics 10(3) (2015) 276-286.

[2] M. E. Dávila, et al., Germanene: a novel two-dimensional germanium allotrope akin to graphene andsilicene, New Journal of Physics 16(9) (2014) 095002.

[3] S.N.Balendhran, et al., Bhaskaran, Elementalanalogues of graphene: silicene, germanene, stanene, and phosphorene small 11(6) (2015) 640-652.

[4] E. S. Kadantsev, and P. Hawrylak, Electronic structure of a single MoS_2 monolayer Solid State Communications 152(10) (2012) 909-913.

[5] K. F. Mak, et al., Atomically thin MoS_2: a new direct-gap semiconductor Physical review letters 105 (13) (2010) 136805.

[6] Y. Zhang, et al., Ambipolar MoS_2 thin flake transistors, Nano Letters *12*(3) (2012) 1136-1140.

[7] B. Radisavljevic, M. B. Whitwick, and A. Kis, Small-signal amplifier based on single-layer MoS_2, Applied Physics Letters, 101(4) (2012) 043103.

[8] L. Fornarini, et al., Electrochemical solarcells with layer-type semiconductor anodes. Performance of n-MoS_2 cells, Solar Energy Materials 5(1) (1981) 107-114.

[9] K. H. Hu, et al., Tribologicalproperties of MoS_2 with different morphologies in high-density polyethylene, Tribology Letters 47(1) (2012) 79-90.

[10] Y. Zhang, et al., Ambipolar MoS_2 thin flake transistors, Nano letters 12(3) (2012) 1136-1140.

[11] B. Radisavljevic, M. B. Whitwick, and A. Kis, Small-signal amplifier based on single-layer MoS_2, Applied Physics Letters 101(4) (2012) 043103.

[12] L. Fornarini, et al., Electrochemical solarcells with layer-type semiconductor anodes. Performance of n-MoS_2 cells, Solar Energy Materials 5(1) (1981) 107-114.

[13] K. H. Hu, et al., Tribological properties of MoS_2 with different morphologies in high-density polyethylene, Tribology Letters 47(1) (2012) 79-90.

[14] H. K. Neupane, and N. P. Adhikari, Structure, electronic and magnetic properties of 2D Graphene-Molybdenum diSulphide (G-MoS_2) Heterostructure (HS) with vacancy defects at Mo sites, Computational Condensed Matter e00489 (2020).

[15] H. K. Neupane, and N. P. Adhikari, Tuning Structural, Electronic, and Magnetic Properties of C Sites Vacancy Defects in Graphene/MoS_2 van der Waals Heterostructure Materials: A First-Principles Study, Advances in Condensed Matter Physics (2020).

[16] H. K. Neupane, and N. P. Adhikari, First-principles study of structure, electronic, and magnetic properties of C sites vacancy defects in water adsorbed graphene/MoS_2 van der Waals Heterostructures, Journal of Molecular Modeling, 27(3) (2021) 1-12.

[17] C. Kittel, P. McEuen, and P. McEuen, Introduction to solid state Physics (Vol. 8, pp. 140-303). New York: Wiley (1996).

[18] A. Splendiani, et al., Emerging photoluminescence in monolayer MoS_2, Nano Letters, 10(4) (2010) 1271-1275.

[19] H. Schmidt, et al., Transport properties of monolayer MoS_2 grown by chemical vapor deposition, Nano Letters, 14(4) (2014)1909-1913.

[20] B. Radisavljevic, and A. Kis, Mobility engineering and a metal–insulator transition in monolayer MoS_2, Nature materials 12(9) (2013) 815-820.

[21] D. P. Rai, et al., Electronic and optical properties of 2D monolayer (ML) MoS_2 with vacancy defect at S sites, Nano-Structures & Nano-Objects 21 (2020) 100404.

[22] P. Hohenberg, and W. Kohn, Inhomogeneous electron gas, Physical Review 136 (3B) (1964): B864.

[23] P.Giannozzi, et al., QUANTUM ESPRESSO: modular and open-source software project for quantum simulations of materials *J*ournal of physics Condensed Matter 21(39) (2009) 395502.

[24] A. Kokalj, XcrySDen-a new program for displaying crystalline structures and electron densities, Journal of molecular Graphics and modeling 17.3-4 (1999) 176-179.

[25] J. P. Perdew, K. Burke, and M. Ernzerhof, Generalized gradient approximation made simple, Physical review letters *77*(18) (1996) 3865.

[26] R. M. Martin, Electronic structure: basic theory andpractical methods, Cambridge University Press (2004).

[27] B. G. Pfrommer, et al., Relaxation of Crystals with the quasi-Newton method, Journal of Computational Physics 131(1) (1997) 233-240.

[28] N. Marzari, et al., Thermal contraction and disordering of the Al (110) surface, Physical Review Letters 82(16) (1999) 3296.

[29] E. S. Kadantsev, and P. Hawrylak, Electronic structure of a single MoS_2monolayer, Solid State Communications 152(10) (2012) 909-913.

[30] S. Ahmad, and S. Mukherjee, A comparative study of electronic properties of bulk MoS2 and its monolayer using DFT technique: application of mechanical strain on MoS2 monolayer (2014).

[31] J. P. Perdew, K. Burke, and M. Ernzerhof, Generalized gradient approximation made simple. Physical Review Letters 77(18) (1996) 3865.

[32] Z. Hou, et al., Interplay between nitrogen dopants and native point defects in graphene, Physical Review B 85 (16) (2012) 165439.